

Winding Angle Distributions for Directed Polymers

Barbara Drossel and Mehran Kardar

Department of Physics, Massachusetts Institute of Technology, Cambridge, Massachusetts 02139

(October 29, 2018)

We study analytically and numerically the winding of directed polymers of length t around each other or around a rod. Unconfined polymers in pure media have exponentially decaying winding angle distributions, the decay constant depending on whether the interaction is repulsive or neutral, but not on microscopic details. In the presence of a chiral asymmetry, the exponential tails become non universal. In all these cases the mean winding angle is proportional to $\ln t$. When the polymer is confined to a finite region around the winding center, e.g. due to an attractive interaction, the winding angle distribution is Gaussian, with a variance proportional to t . We also examine the windings of polymers in random systems. Our results suggest that randomness reduces entanglements, leading to a narrow (Gaussian) distribution with a mean winding angle of the order of $\sqrt{\ln t}$.

I. INTRODUCTION AND SUMMARY

The topological constraints produced by the windings of polymers [1] strongly affect the dynamics of polymer solutions. As a consequence of polymer entanglement, the viscosity of a solution of polymers above the overlap concentration is many orders of magnitude higher than the viscosity of the solvent. An analytical treatment of these topological constraints is extremely difficult, and theoretical efforts therefore focus on the limit of high polymer concentrations, where effective medium theories and the tube model successfully describe several aspects of the dynamics of the polymer solution [2], or on the limit of only one or two polymers, where the different possible configurations can be studied explicitly [3].

In this article, we take the latter approach, focussing on the winding of a directed polymer

(DP) around a rod, or of two DPs around each other, as shown in Fig. 1. DPs have a preferred direction $\hat{\tau}$, and their configuration can be described by the function $\{\vec{r}(\tau)\}$, with $\tau \in [0, t]$, where $\vec{r} = (x_1, x_2)$ is the coordinate in the plane perpendicular to the preferred direction. Going to relative coordinates $\vec{r}_2(\tau) - \vec{r}_1(\tau)$, the winding of two DPs around each other can be mapped to the winding of a single DP around a rod (see section II). Since DPs cannot have knots, their main topological constraints are windings.

Although less common than flexible polymers, DPs are a good model of several semi-flexible and rigid polymers. Examples are biological macromolecules such as DNA or liquid crystals composed of stacks of disk-shaped molecules. These polymers are aligned parallel to each other when their concentration is sufficiently large, forming crystalline and liquid crystalline phases (for a review on statistical mechanics of DPs see e.g. [4]). Isolated DPs can be realized by embedding a long polymer in a nematic solvent [5]. Another important class of directed “polymers” are magnetic flux lines in high- T_c superconductors that are oriented parallel to the direction of the external magnetic field. Due to the high temperature in the system and the weak coupling between different layers in the superconductor, thermal fluctuations of the flux lines are considerable, leading to entanglements [6,7] and windings around columnar pins [8].

In order to calculate the winding angle distribution of DPs, we map them onto two-dimensional walks $\{\vec{r}(\tau)\}$, where the arc length τ plays the role of the time coordinate. The winding angle distribution depends on the interaction between the polymer and the winding center, and the properties of the embedding medium. In the following three sections, we discuss three different classes of winding angle distributions, for each of which the scaling variable is a different combination of the winding angle θ and the polymer length t . In section II, we consider DPs in an infinitely large pure medium. These polymers can be mapped on ideal random walks, the mean horizontal distance $\langle |\vec{r}(\tau) - \vec{r}(0)| \rangle$ from the starting point increasing with the square root of τ . The number of returns to the winding center is proportional to $\ln t$ for such a random walk. We will see below that because of the finite return probability to the winding center even for large times, the winding angle

distribution depends on properties of the winding center. We will find different winding angle distributions depending on whether the interaction between the winding center and the polymer is a hard-core repulsion or is neutral, and whether the winding center shows a chiral asymmetry. However, the winding angle distribution does not depend on microscopic details like the shape of the winding center or a possible underlying lattice structure. The probability distribution for the winding angle depends in the limit $t \rightarrow \infty$ only on the combination $x = 2\theta/\ln(t)$ of the winding angle and the length of the walk, and not on each variable separately. For large $|x|$, all three mentioned winding angle distributions decay exponentially in $|x|$. The scaling variable proportional to $\theta/\ln(t)$ can be explained as follows: After time t , the walker has a typical distance $r(t) \propto \sqrt{t}$ from the starting point, which is chosen to be close to the winding center. Assuming that $r(t)$ is the only relevant length scale, dimensional arguments, combined with the Markovian property, suggest that $dr/d\theta = rf(\theta)$. The rotational invariance of the system implies that $f(\theta)$ must be a constant, i.e. the increase in winding angle cannot depend on the number of windings or angular position. Hence,

$$d\theta \propto \frac{dr}{r} \propto \frac{dt}{t} = d(\ln t), \quad (1)$$

leading to a scaling variable proportional to $\theta/\ln t$.

If the interaction between the polymer and the winding center is attractive, the polymer can be bound to the winding center, and its transverse wandering is limited. Polymers can also be confined by a finite container or by neighboring polymers. In all these cases, polymer segments of length Δt that are small compared to the total length t , but large compared to the length needed to make a winding, have identical winding angle distributions. Applying the central limit theorem, we conclude that the total winding angle distribution is a Gaussian with a scaling variable θ^2/t . This situation will be discussed in section III.

Finally, we discuss in section IV certain DPs that cannot be described by ideal random walks, since they do not satisfy a Markov property. Polymers that are embedded in a random medium, e.g. a gel, have an energy that depends on the polymer configuration. Similarly,

the energy of magnetic flux lines in high- T_c superconductors with point defects depends on their configuration. The mean distance from the starting point for these polymers in random media increases faster than for ideal walks, since the line searches for low-energy configurations. The number of returns to the winding center remains finite in the limit of infinite length. Consequently, the interaction of the line with the winding center does not affect the winding angle distribution, as long as it is not strong enough to bind the polymer. We will see that the winding angle distribution of polymers in random media is a Gaussian with a variance proportional to $\ln t$, leading to a scaling variable $x \propto \theta/\sqrt{\ln(t)}$. This means that the pinning to randomness decreases the mean winding angle from the order of $\ln t$ to the order of $\sqrt{\ln t}$. Interestingly, this winding angle distribution is similar to the one for two-dimensional self-avoiding random walks [9]. The following scaling argument explains why the winding angle distribution in both situations is Gaussian with a variance proportional to $\ln t$: Starting from the origin divide the walk into segments of $1, 2, \dots, 2^n \approx t/2$ steps. Since the α^{th} segment is at a distance of roughly $2^{\alpha\nu}$ from the center (with $\nu = 3/4$) and has a characteristic size of the same order, it is reasonable to assume that each segment spans a random angle θ_α of order one. Under the mild assumption that the sum $\theta = \sum_{\alpha=1}^n \theta_\alpha$ satisfies the central limit theorem, we then conclude that θ is Gaussian distributed with a variance proportional to $n \propto \ln t$. Since this argument relies on the irrelevance of the winding center, it cannot be applied to the distributions in section II.

Many results of this article have been reported previously in Ref. [10]. They point out the rich behavior already present in the simplest of problems involving topological defects. Properties of the winding center, interactions, various types of randomness are all potentially relevant, leading to different universal distribution functions. The concluding section V of this article gives an outlook on possible further universality classes and on the winding of non-directed polymers.

II. WINDING ANGLE DISTRIBUTIONS IN AN INFINITE HOMOGENEOUS MEDIUM

In this section, we study winding angle distributions of DPs in infinite homogeneous media, all characterized by a scaling variable $x = 2\theta/\ln t$ and exponential tails. We keep the initial point of the polymers fixed, but otherwise allow them to move freely. The precise form of the winding angle distribution depends on the interaction with the winding center. In subsection II A, we consider two DPs with hard-core repulsion, or, equivalently, one DP winding around a repulsive rod, leading to the distribution in Eq. (14). For neutral winding centers, the corresponding winding angle distribution given in Eq. (17) has a decay constant that is smaller by one half (subsection II B). These two distributions occur under fairly general conditions (see subsection II C). However, when the symmetry with respect to the sign of the winding angle is broken, new (asymmetric) distributions occur (subsection II D), with the decay constants of the exponential tails depending on the degree of chirality.

A. Winding in the presence of hard-core repulsion

1. Mapping to a random walk with absorbing boundary conditions

The energy of a given configuration of two DPs $\vec{r}_1(\tau)$ and $\vec{r}_2(\tau)$ of length t is given by

$$E[\vec{r}_1(\tau), \vec{r}_2(\tau)] = \int_0^t d\tau \left[c \left(\frac{d\vec{r}_1}{d\tau} \right)^2 + c \left(\frac{d\vec{r}_2}{d\tau} \right)^2 + V(\vec{r}_1 - \vec{r}_2) \right]. \quad (2)$$

The potential $V(\vec{r})$ has a hard-core, $V(r) = \infty$ for $r < a$, and $V(r) = 0$ for $r > a$. The first two terms are the elastic energies of the polymers, where the parameter c is related to their stiffness. Introducing the relative coordinate $\vec{r} = \vec{r}_1 - \vec{r}_2$ and the center-of-mass coordinate $\vec{R} = (\vec{r}_1 + \vec{r}_2)/2$, Eq. (2) becomes

$$E[\vec{R}(\tau), \vec{r}(\tau)] = \int_0^t d\tau \left[\frac{c}{2} \left(\frac{d\vec{r}}{d\tau} \right)^2 + 2c \left(\frac{d\vec{R}}{d\tau} \right)^2 + V(\vec{r}) \right].$$

The partition function for the two polymers is

$$Z = \int \mathcal{D}[\vec{R}(\tau)] \mathcal{D}[\vec{r}(\tau)] \exp \left\{ -E[\vec{R}(\tau), \vec{r}(\tau)] / k_B T \right\}, \quad (3)$$

where the integral is taken over all possible configurations $[\vec{R}(\tau)]$ and $[\vec{r}(\tau)]$. The expression $\mathcal{D}[\vec{r}(\tau)]$ denotes a path integral and is the continuum limit of $\prod_{i=1}^n (\int d\vec{r}(\tau_i))$, k_B is the Boltzmann constant, and T is the temperature.

As long as we are only interested in quantities related to the relative coordinate, like the winding angle, we can integrate out the center-of-mass variations, and focus on the partition function for the relative coordinate alone, i.e.,

$$Z = \int \mathcal{D}[\vec{r}(\tau)] \exp \left\{ - \int_0^t d\tau \left[\frac{c}{2} \left(\frac{d\vec{r}}{d\tau} \right)^2 + V(\vec{r}) \right] / k_B T \right\}. \quad (4)$$

This is identical to the partition function for a single DP winding around a rod. Due to the hard-core repulsion, all configurations where the polymer and the rod penetrate each other, do not contribute to the partition function ($V = \infty$), while $V = 0$ for all other configurations.

A two-dimensional random walk can be described by the Langevin-equation

$$\frac{d\vec{r}}{dt} = \vec{\eta}(t), \quad (5)$$

where η is a stochastic force with zero mean ($\langle \eta(t) \rangle = 0$) and the correlation function $\langle \vec{\eta}(t) \vec{\eta}(t') \rangle = 2D\delta(t - t')$. The probability distribution of $\vec{\eta}$ is a Gaussian, i.e.

$$P[\eta(t)] \propto \exp \left[-D (\vec{\eta}(t))^2 \right].$$

With Eq. (5), we find that the probability for a given trajectory $[\vec{r}(\tau)]$ of the random walk is proportional to

$$\exp \left\{ - \int_0^t d\tau \left[D \left(\frac{d\vec{r}}{d\tau} \right)^2 \right] \right\}.$$

When all walks that enter a region of radius a around the origin get absorbed, the probability that the random walk has a trajectory $[\vec{r}(\tau)]$ is identical to the probability that the above DP has the configuration $[\vec{r}(\tau)]$ (compare to Eq. (4), with $D = c/k_B T$). This correspondence between DPs with hard-core repulsion and random walks with absorbing boundary conditions was first pointed out by Rudnick and Hu [11].

2. Conformal mapping of the random walk

Since we are interested in the winding angle of the random walk, it is convenient to perform a transformation such that the winding angle becomes one of the coordinates. To this purpose, we represent the walk $\vec{r}(t) = (x_1(t), x_2(t))$ by the complex number

$$z(t) = x_1(t) + ix_2(t).$$

The time evolution of each random walker satisfies

$$dz = \eta(t)dt, \quad (6)$$

where $\eta(t)$ is now complex, with

$$\langle \eta(t)\eta^*(t') \rangle = 2D\delta(t - t'). \quad (7)$$

We now introduce the new variable ζ by the transformation

$$\zeta(t) = \ln z(t) = \ln r(t) + i\theta(t), \quad (8)$$

where $\rho = \ln r = \ln \sqrt{x_1^2 + x_2^2}$. Since $d\zeta = \eta(t)dt/z(t)$, the stochastic motion of the walker in the new complex plane is highly correlated to its location, i.e., the walk is no longer random. This feature can be removed by defining a new time variable

$$d\tilde{t} = \frac{dt}{|z(t)|^2} \quad (9)$$

for each walker, which leads to

$$d\zeta = \mu(\tilde{t})d\tilde{t}, \quad \text{with} \quad \mu(\tilde{t}) = z^*(t)\eta(t). \quad (10)$$

Since

$$\langle \mu(\tilde{t})\mu^*(\tilde{t}') \rangle = 2D|z(t)|^2\delta(t - t') = 2D\delta(\tilde{t} - \tilde{t}'), \quad (11)$$

the evolution of $\zeta(\tilde{t})$ is that of a random walk. Under the transformation in Eq. (8), the absorbing disc in the plane z maps onto an absorbing wall in the plane ζ (see Fig. 2).

For simplicity we choose the initial condition $\zeta(t = \tilde{t} = 0) = 0$, i.e. the original walker starts out at $z = 1$. We also set the diffusion constant to $D = 1/2$, so that the mean square distance over which the walk moves during a time t is $\langle r^2(t) \rangle = t$. Consequently, the probability that $r(t)$ is within an interval $[\sqrt{\pi}t^{(1-\epsilon)/2}, \sqrt{\pi}t^{(1+\epsilon)/2}]$ around its mean value of $\sqrt{\pi}t$, is

$$\begin{aligned} p(t, \epsilon) &= \int_{\sqrt{\pi}t^{(1-\epsilon)/2}}^{\sqrt{\pi}t^{(1+\epsilon)/2}} \frac{\exp(-r^2/2t)}{2\pi t} 2\pi r dr \\ &= \int_{\pi t^{-\epsilon/2}}^{\pi t^{\epsilon/2}} \exp(-s) ds, \end{aligned} \quad (12)$$

and approaches unity in the limit $t \rightarrow \infty$. The effect of the absorbing disc on this probability can be neglected in the limit $t \rightarrow \infty$, since the disc becomes smaller when viewed from larger distances. In this limit, the distance r from the starting point $z = 1$ is identical to the distance from the origin, and $p(t, \epsilon)$ is identical to the probability that $\zeta(\tilde{t})$ is in the interval $[0.5(1 - \epsilon) \ln t, 0.5(1 + \epsilon) \ln t]$. So the endpoints of all walks (except for an infinitesimal fraction) that take a time t in the original plane map within a strip of width $\epsilon \ln t$ in the ζ -plane, as indicated in Fig. 2. If we shrink the complex plane ζ by a factor of $(\ln t)/2$, the walker is within a distance ϵ of the line with real value of unity. Thus, all walks of length t in the z -plane are mapped on walks that end at the line with real value of unity, without having gone beyond (see Fig. 2). Since there is a separate transformation $\tilde{t}(t)$ for each walker, walks of the same length t map on walks of different length \tilde{t} . (To be precise, we also have to shrink the time scale \tilde{t} when shrinking the ζ -plane, but for simplicity we denote the new time again by \tilde{t} .)

3. Calculation of the winding angle distribution

The imaginary (or vertical) coordinate x in the rescaled ζ -plane is related to the winding angle by $x = 2\theta(t)/\ln t$. In order to obtain the winding angle distribution, we have to determine the vertical position of a random walk starting at the origin, at the moment when it reaches for the first time the wall at distance one from the vertical axis, without

going beyond the absorbing wall at distance $2|\ln a|/\ln t$ on the opposite side. Since we are interested in a walk only up to the moment when it reaches the right-hand wall, we can consider this wall also as absorbing. Since walks of length t in the original plane map on walks of different length \tilde{t} in the new plane, we need the probability that the walk is absorbed at this wall before time \tilde{t} .

We formulate this problem more generally and determine the probability $P_{\alpha,\beta}(y, \tilde{t})$ that a one-dimensional random walk starting at y between two absorbing points α and β at time 0 is absorbed at the point β before time \tilde{t} . Since for sufficiently small $\Delta\tilde{t}$, the walker is only a short distance Δy from its starting point, we have

$$P_{\alpha,\beta}(y, \tilde{t}) = \int_0^\infty d(\Delta y) \frac{1}{\sqrt{2\pi\Delta\tilde{t}}} \exp\left[-\frac{(\Delta y)^2}{2\Delta\tilde{t}}\right] \times [P_{\alpha,\beta}(y + \Delta y, \tilde{t} - \Delta\tilde{t}) + P_{\alpha,\beta}(y - \Delta y, \tilde{t} - \Delta\tilde{t})].$$

Expanding the above equation to the order of $\Delta\tilde{t}$ indicates that $P_{\alpha,\beta}(y, \tilde{t})$ satisfies a diffusion equation. The appropriate boundary conditions are $P_{\alpha,\beta}(\alpha, \tilde{t}) = 0$ and $P_{\alpha,\beta}(\beta, \tilde{t}) = 1$ with the initial value $P_{\alpha,\beta}(y, 0) = 0$, resulting in [12]

$$P_{\alpha,\beta}(y, \tilde{t}) = \frac{y - \alpha}{\beta - \alpha} + \frac{2}{\pi} \sum_{\nu=1}^{\infty} \frac{(-1)^{\nu+1}}{\nu} \sin\left(\frac{\pi\nu(y - \alpha)}{\beta - \alpha}\right) \times \exp\left[-\frac{1}{2} \left(\frac{\pi\nu}{\beta - \alpha}\right)^2 \tilde{t}\right].$$

The probability that the walk is absorbed at the right-hand boundary during the time interval $[\tilde{t}, \tilde{t} + d\tilde{t}]$, is $d\tilde{t} \partial_{\tilde{t}} P_{\alpha,\beta}(y, \tilde{t})$.

Note, however, that $\int_0^\infty d\tilde{t} \partial_{\tilde{t}} P_{\alpha,\beta}(y, \tilde{t}) = (y - \alpha)/(\beta - \alpha)$, i.e. equal to the total fraction of particles absorbed at the right-hand boundary (inversely proportional to the separations from the boundaries). To calculate the winding angle distribution $p_A(x)$, we need the fraction of these walks absorbed between \tilde{t} and $\tilde{t} + d\tilde{t}$, equal to $((\beta - \alpha)/(y - \alpha)) \partial_{\tilde{t}} P$. Hence (with $\alpha = 2 \ln a / \ln t$, $\beta = 1$ and $y = 0$)

$$p_A(x) = \int_0^\infty d\tilde{t} \frac{1 - \alpha}{-\alpha} \frac{\partial P_{\alpha,1}(0, \tilde{t})}{\partial \tilde{t}} \frac{\exp(-x^2/2\tilde{t})}{\sqrt{2\pi\tilde{t}}}$$

$$\begin{aligned}
&= \int_0^\infty d\tilde{t} \sum_{\nu=1}^{\infty} \frac{(-1)^{\nu+1}}{\sqrt{2\pi\tilde{t}}} \frac{\pi\nu}{\alpha(1-\alpha)} \sin\left(\frac{\pi\nu\alpha}{1-\alpha}\right) \\
&\quad \times \exp\left[-\frac{1}{2}\left(\frac{\pi\nu}{1-\alpha}\right)^2 \tilde{t} - \frac{x^2}{2\tilde{t}}\right] \\
&= \sum_{\nu=1}^{\infty} \frac{(-1)^{\nu+1}}{\alpha} \sin\left(\frac{\pi\nu\alpha}{1-\alpha}\right) \exp\left[-\frac{\pi\nu|x|}{(1-\alpha)}\right].
\end{aligned}$$

The last step is achieved by first performing a Fourier transform with respect to x , followed by integrating over \tilde{t} , and finally inverting the Fourier transform. (Alternatively, the \tilde{t} integration can be performed by the saddle point method.) In the limit of large t , the variable α is very small, and we can replace the sine-function by its argument.

Taking the sum over ν , we find

$$p_A(x) = \frac{\pi}{(1-\alpha)} \frac{\exp[\pi x/(1-\alpha)]}{\{\exp[\pi x/(1-\alpha)] + 1\}^2}. \quad (13)$$

Changing the variable from x to

$$\tilde{x} = \frac{x}{(1-\alpha)} = \frac{2\theta}{\ln(t/\alpha^2)},$$

and noting that $p_A(x)dx = p_A(\tilde{x})d\tilde{x}$, leads from Eq. (13) to

$$p_A\left(\tilde{x} = \frac{2\theta}{\ln(t/\alpha^2)}\right) = \frac{\pi}{4\cosh^2(\pi\tilde{x}/2)}. \quad (14)$$

The above distribution, which is exact in the limit $t \rightarrow \infty$, has an exponential decay for large \tilde{x} , as first derived in Ref. [11]. The complete form of Eq. (14) was first given in Ref. [13], however, without derivation. The analogy to random walkers in the plane ζ , confined by the two walls, provides simple physical justifications for the behavior of the winding angle. In the presence of both walls, the diffusing particle is confined to a strip, and loses any memory of its starting position at long times. The probability that a particle that has already traveled a distance θ in the vertical direction proceeds a further distance $d\theta$ without hitting either wall is thus independent of θ , leading to the exponential decay.

4. Comparison to the winding angle distribution around a point center

The method described in this section was used earlier to derive the winding angle distribution for Brownian motion around a point center [14]. The resulting probability distribution for the winding angle in this case is [15]

$$\lim_{t \rightarrow \infty} p \left(x = \frac{2\theta}{\ln t} \right) = \frac{1}{\pi} \frac{1}{1+x^2}, \quad (15)$$

leading to an infinite mean winding angle. Since there is no confining wall on the left-hand side, the particles may diffuse arbitrarily far in that direction, making it less probable to hit the wall on the right hand side. In the original z -plane, the walker takes no time at all to make an infinitely small winding around the point center. This is clearly an unphysical feature, since real winding centers are finite and since real random walks (or polymers) need a finite time (a finite length segment) to make a winding. We therefore do not consider this situation any further.

Exercise: Derive Equation (15), repeating the calculation of this section, but with no absorbing wall (see Ref. [10]).

B. Winding of directed polymers around neutral winding centers

Instead of having first a rod and then inserting the DP into the system, we can also first have a free configuration of a DP, and then insert a rod into it. If the polymer cannot relax to its thermal equilibrium distribution after insertion of the rod, e.g. because its end are fixed or because its configuration is frozen, the resulting winding angle distribution will be different from that in the previous subsection. No configuration of the polymer is forbidden, but those configurations that interfere with the rod become *deformed*. The degree of deformation may depend on the diameter of the rod, but the winding angle does not. Alternatively, we could consider a winding center that has no interaction at all with the polymer, e.g. a light beam, or some structural defect in the solvent that is not felt by the polymer. In this case we would find the same winding angle distribution as in the case of a

rod that deforms the polymer. In the language of a random walk, this situation corresponds to having a disc that reflects all walks that hit it. The walks that would go through the disc thus become deformed, but are not removed from the statistical ensemble.

We can obtain the winding angle distribution by repeating the calculations of the previous subsection, but replacing the absorbing boundary condition $P_{\alpha,\beta}(\alpha, \tilde{t}) = 0$ with the reflecting condition $\partial P_{\alpha,\beta}(y, \tilde{t})/\partial y|_{y=\alpha} = 0$, leading to

$$P_{\alpha,\beta}(y, \tilde{t}) = 1 - \frac{2}{\pi} \sum_{\nu=0}^{\infty} \frac{1}{\nu + 1/2} \sin \left(\frac{\pi(\nu + 1/2)(\beta - y)}{\beta - \alpha} \right) \times \exp \left[-\frac{1}{2} \left(\frac{\pi(\nu + 1/2)}{\beta - \alpha} \right)^2 \tilde{t} \right]. \quad (16)$$

There is thus no current leaving the system at point α , and walkers which hit the winding center are reflected. We then find the winding angle distribution

$$p_R(\tilde{x}) = \frac{1}{2 \cosh(\pi \tilde{x}/2)}, \quad (17)$$

where again $\tilde{x} = 2\theta/\ln(t/a^2)$, and the limit $t \rightarrow \infty$ has been taken. For large \tilde{x} , where the walk has lost the memory of its initial distance from both walls, this probability decays exponentially as $\exp[-\pi \tilde{x}/2]$, i.e. exactly half as fast as for absorbing boundary conditions. A random walk confined between an absorbing and a reflecting wall that have a distance one can be mapped to a random walk confined between two absorbing walls at distance two. After rescaling the wall distance and the \tilde{x} -coordinate by two, this explains the factor $1/2$ between the decay constants in the tails of the distributions in Eqs. (14) and (17).

Exercise: Derive Equation (17) (see Ref. [10]).

C. Universality of the winding angle distribution

The winding angle distribution in Eq. (17), which we derived in the previous subsection for Brownian motion around a reflecting disc, was obtained previously by several authors in different contexts: Bélisle [16] calculated the winding angle distribution for a random walk on a two-dimensional lattice around a point that is different from any lattice site, and for

a random walk with steps of finite size taken in arbitrary directions, around a point in the two-dimensional plane, obtaining in both cases Eq. (17). The same result was obtained by Pitman and Yor [17] for the distribution of “big windings” of Brownian motion around two point-like winding centers. Comtet, Desbois, and Monthus [18] divided the two-dimensional plane into three concentric sections and determined the contribution of each section to the winding angle for Brownian motion around a point, finding Eq. (17) for the contribution of the outer section. This universality seems surprising, since one might expect that the main increase in winding angle occurs when the walk is close to the winding center, where details like the lattice symmetry, and shape and size of the winding center determine how much time it takes to make one winding. However, a careful look at Fig. 2 reveals that this is not the case: The main increase in winding angle does not occur when the walker is within a small distance from the left-hand wall. Since all distances have been scaled by $1/\ln(t)$, a small distance from the left-hand wall corresponds to a large distance (of the order of $\ln t$) from the winding center. Therefore, almost all windings are made far from the winding center, where microscopic details do not matter. The properties that do affect the winding angle distribution are conservation laws (absorbing or reflecting boundary conditions), symmetries (with respect to the sign of the angle - see the following subsection), singularities (as for the winding of Brownian motion around a point center), and interactions (self-avoidance) or randomness (see section IV).

To further test this universality hypothesis, we determined numerically the winding angle distribution for a random walk on a lattice with reflecting and absorbing boundary conditions. Reflecting boundary conditions are realized by choosing a winding center different from the vertices of the lattice, and thus never crossed by the walker (this is exactly the situation treated analytically in Ref. [16]). On the other hand, to model absorbing boundary conditions, the winding center is chosen as one of the lattice sites (say the origin), but no walk is allowed to go through this point.

The winding angle distributions are most readily obtained using a transfer matrix method which calculates the number of all walks with given winding angle and given endpoint after

t steps, from the same information after $t - 1$ steps. The winding center is at $(0.5, 0.5)$ for reflecting boundary conditions, and at the origin for absorbing boundary conditions. The walker starts at $(1,0)$, and the winding angle is increased or decreased by 2π every time it crosses the positive branch of the x_1 -axis. Due to limitations in computer memory, we applied a cutoff in system size and winding angle for times $t > 120$, making sure that the results are not affected by this approximation. The largest times used, $t = 9728$, required approximately 3 days to run on a Silicon Graphics Indy Workstation.

Figures 3 and 4 show the results for the two cases. The asymptotic exponential tails predicted by theory can clearly be seen; deviations from the theoretical curve for smaller values of the scaling variable $x = 2\theta/\ln(2t)$ are due to the slow convergence to the asymptotic limit. Since the scaling variable depends logarithmically on time, the asymptotic limit is reached only for large $\ln t$. Note that the only free parameter in fitting to the analytical form is the characteristic time scale appearing inside the logarithm. With t measured in units of single steps on the lattice, we found that a factor 2 in the scaling variable provides the best fit. In the limit $t \rightarrow \infty$, different scales of t give of course the same asymptotic winding angle distribution.

Exercise: Perform the numerical calculations mentioned in this section. Study also the case of absorbing and reflecting winding centers that comprise several lattice points. How does the size of the winding center affect the convergence towards the asymptotic winding angle distribution?

We also studied the winding of a DP proceeding along the diagonal of a cubic lattice in three dimensions (see Fig. 5). The polymer starts at $(1, 0, 0)$, and at each step increases one of its three coordinates by 1. We determined the winding angle distribution around the diagonal $(1, 1, 1)$ -direction, excluding from the walk all points that are on this diagonal (a repulsive columnar defect, corresponding to the case of an absorbing winding center). The excluded points lie on the origin when the polymer is projected in a plane perpendicular to the diagonal. In this plane, the polymer proceeds along the bonds of a triangular lattice, alternating between the three different sublattices. A cutoff of 243 in system size was imposed

for the transfer matrix calculations. The winding angle distribution $p(x = 2\theta/\ln t)$ is shown in Fig. 6 for different times. As for the square lattice, an exponential tail with decay constant of π can be seen. Our numerical results, as well as the analytical considerations, thus indicate clearly that the winding angle distributions for reflecting and absorbing boundary conditions are universal and do not depend on microscopic details.

Due to the special properties of directed paths along the diagonal of the cube, the case of reflecting boundary conditions leads to an asymmetry between windings in positive and negative directions. This is because it takes only three steps to make the smallest possible winding in one direction, but six steps in the opposite direction. This situation is discussed in detail in the following subsection.

D. Winding centers with chiral asymmetry

So far, we only considered situations that are symmetric with respect to the angles $\pm\theta$. For directed paths on certain lattices, however, this symmetry is broken. A directed walk that proceeds at each step along $+x_1$, $+x_2$, or $+x_3$ direction on a cubic lattice can be mapped on a random walker on a two-dimensional triangular lattice as indicated in figure 7(a). Each bond can be crossed only in one direction, and the winding center for reflecting boundary conditions must be different from the vertices of the lattice. It is apparent from this figure that the random walker can go around the center in 3 steps in one angular direction, but in no less than 6 steps in the other direction.

An alternative description is obtained by examining the position of the walker after every three time steps. The resulting coarse-grained random walk takes place on a regular triangular lattice, but now the walker has a finite probability of $3 \times 2/3^3 = 2/9$ of staying at the same site. If this site is one of the three points next to the winding center, the winding angle is increased by 2π in one of the six possible configurations that return to the site after three steps. In other words, the walker has a finite probability of having its winding angle increased in the proximity of the center. The amount of this biased increase in angle

depends on the structure of the lattice and will be different for other directed lattices. An equivalent physical situation occurs for Brownian motion around a rotating winding center, e.g. a rotating reflecting disc which does not set the surrounding gas or liquid into motion (see Fig. 8).

Since this angular symmetry breaking is already present in the above simple example of a directed walk, it is quite likely to occur in more realistic physical systems, such as with screw dislocations in the underlying medium. The winding angle distribution for two *chiral* polymers [5] should also show an angular asymmetry. We thus use the term chiral winding center to indicate that each time the polymer comes close to the center, it finds it easier to wind around in one direction as opposed to the other. (Of course, to respect the reflecting boundary conditions, there must be no additional interaction with the winding center. The case of additional attractive or repulsive interaction with the winding center will be discussed later.)

After mapping to the rescaled ζ -plane introduced in Sec. II, the above situations can be modeled by a downward moving, reflecting wall on the vertical axis. Each time a random walker hits this wall, its vertical position $x = 2\theta/\ln t$ is changed by a small amount $2\Delta\theta/\ln t$. Let us now determine the net shift Δx in x due to the motion of the wall for a walker that survives for a time \tilde{t} in the rescaled ζ -plane, before it is absorbed at the right-hand wall (recall that t is the time in the original system, while \tilde{t} refers to the time in the rescaled ζ -plane, after the conformal mapping).

To obtain the full solution, it is necessary to solve the two-dimensional diffusion equation with moving boundary conditions. Since we are mainly interested in the exponential tails of the winding angle distribution, we restrict our analysis to the limit of large times \tilde{t} , and determine the shift in x due to encounters with the reflecting moving wall in this limit. A Brownian walker that has survived for a sufficiently long time \tilde{t} forgets its initial horizontal position. The mean number of encounters with the reflecting wall, and consequently the shift Δx in x due to the motion of the wall, is then expected to be simply proportional to the considered time interval. Applying the central limit theorem in the limit $\tilde{t} \rightarrow \infty$, the

probability distribution of Δx is given by

$$p_\Delta(\Delta x) = \frac{1}{\sqrt{2\pi\beta^2\tilde{t}}} \exp\left[-\frac{(\Delta x - \alpha\tilde{t})^2}{2\beta^2\tilde{t}}\right]. \quad (18)$$

The parameters α and β are related to the velocity of the wall (chirality of the defect) by $\alpha \propto \beta \propto v$. Presumably Eq. (18) can be obtained directly from properties of random walks, providing the exact coefficients for these proportionalities.

The tail of the winding angle distribution is then given by

$$\begin{aligned} p_R^c(x) &\propto \int_0^\infty d\tilde{t} \int_{-\infty}^\infty d(\Delta x) \frac{\partial P_{\alpha,1}(0,\tilde{t})}{\partial \tilde{t}} \frac{1}{\sqrt{2\pi\tilde{t}}} \exp\left[-\frac{(x - \Delta x)^2}{2\tilde{t}}\right] \\ &\propto \int_0^\infty d\tilde{t} \exp\left[-(\pi^2/4)\tilde{t}/2\right] \frac{1}{\sqrt{2\pi\tilde{t}(1+\beta^2)}} \exp\left[-\frac{(x - \alpha\tilde{t})^2}{2\tilde{t}(1+\beta^2)}\right] \\ &= \exp\left[\frac{\alpha x}{1+\beta^2} - \frac{|x|}{1+\beta^2} \sqrt{\alpha^2 + \frac{\pi^2}{4}(1+\beta^2)}\right], \end{aligned} \quad (19)$$

valid for large $|x|$. The second factor on the right-hand side of the first line of Eq. (19) is the probability that the random walker is absorbed at the right-hand wall at time \tilde{t} (see Eq. (16), and is for large \tilde{t} dominated by the slowest mode ($\nu = 0$). The second factor is the probability that the random walk would have the vertical coordinate x after time \tilde{t} , if there were no motion of the wall. The effect of the moving wall on the winding angle distribution is thus a systematic shift in the slopes of the exponential tails. For small values of chirality the slopes on the two sides are changed to $\pi/2 \pm \alpha$. Due to this explicit velocity dependence, these asymmetric distributions are clearly non-universal. At large chiralities, the slopes vanish as α/β^2 resulting in quite wide distributions. Apparently strong chirality of a defect increases the probability of entanglements. Fig. 9 shows our simulation results for the winding angle distribution for a walk on the above mentioned directed triangular lattice. The asymmetry due to the shift is clearly visible, and the winding angle distribution is wider than for a stationary wall. This case thus exemplifies the strong chirality limit discussed in the previous paragraph. We also simulated a square lattice with directed bonds as indicated in Fig. 7(b). The corresponding winding angle distribution is shown in Fig. 10.

The distribution is again asymmetric, but not as wide as in the previous case, and more similar to that expected in the weak chirality regime.

So far, we have assumed that the winding angle changes by the same amount each time the walker returns to the winding center. It is more realistic to assume that the change in winding angle has a certain probability distribution. A possible example is provided by polymers with randomly changing chirality [19]. In the limit $t \rightarrow \infty$, the total change in winding angle due to the chirality is on an average

$$\langle \Delta\theta \rangle = \int_{-\infty}^{\infty} d(\Delta\theta) p(\Delta\theta) \Delta\theta,$$

where $p(\Delta\theta)$ is the probability distribution for $\Delta\theta$. The variance for the total change in the scaling variable x is

$$(\delta\Delta x)^2 \simeq \ln t \left(\frac{2\delta\Delta\theta}{\ln t} \right)^2$$

and vanishes in the limit $t \rightarrow \infty$. The effect of random chirality of the winding angle distribution is identical to that of uniform chirality, and is zero when segments of positive and negative chirality occur equally often.

Finally, we want to emphasize that the results of this section are based on the assumption that there is no interaction between the polymer and the winding center besides the chirality. When there is an additional repulsive interaction, we have to choose absorbing boundary conditions, in which case the random walk never hits the moving wall, and the motion of the wall (the chirality) has no effect at all on the winding angle distribution. On the other hand, when the polymer is bound to the winding center due to an attractive interaction, the number of returns to the winding center, and consequently the systematic shift in the winding angle due to chirality are proportional to the length t (see section III). In the presence of both an attractive interaction and a hard-core repulsion (probably the most realistic case [20]), the polymer performs a phase transition from a bound to a free state depending on the temperature, and we expect the results of this subsection to apply near the transition temperature.

III. THE WINDING ANGLE DISTRIBUTION OF CONFINED POLYMERS

Up to now, we considered only cases where the polymer could wander infinitely far away from the winding center. However, there are many physical situations where polymers indeed are confined to some region around the winding center. When the diameter of the container is small compared to the length of a DP, or when the polymer density is so large that for each of them just a small cylinder is available, the winding angle distribution will be fundamentally different from the previous section. Random walk segments of time Δt that are small compared to the total length of the walk, but large compared to the time it takes to make a winding, have identical winding angle distributions. Applying the central limit theorem, we can therefore predict that the total winding angle distribution of a confined polymer has the form

$$p_{con}(\theta) \propto \exp \left[-a\theta^2/2t \right], \quad (20)$$

where $1/a$ is the variance in the winding angle per unit time.

When the winding center is chirally asymmetric, there is an additional shift in the mean winding angle. In the following three subsections, we will determine the winding angle distribution for polymers confined between two cylinders, polymers bound to an attractive winding center, and bound polymers winding around chiral centers.

A. Polymer confined between two cylinders

We start with the simple model of a polymer confined between two concentric cylinders (see Fig. 11). The inner cylinder is the winding center, the outer one is the wall of the container, or represents the repulsion of the neighboring polymers. This situation is equivalent to a random walk confined between two concentric rings of radii R_1 and R_2 . After a long time, the probability $p(r)$ to find the walker at a given radius r is independent of time, and of the angle. For reflecting boundary conditions at the outer and the inner ring, the walker

is then with equal probability at any site between the two rings, leading to

$$p(r) = \frac{1}{r \ln(R_2/R_1)}.$$

The variance of the winding angle per unit time is $1/r^2$ when the walker is at radius r . Since the variances of different segments of the random walk are independent, we can add them up, leading in the limit of large t to

$$\frac{1}{a} = \int_{R_1}^{R_2} \frac{1}{r^2} p(r) dr = \int_{R_1}^{R_2} \frac{dr}{r^3 \ln(R_2/R_1)} = \frac{t}{2 \ln(R_2/R_1)} \left(\frac{1}{R_1^2} - \frac{1}{R_2^2} \right).$$

It is more physically relevant to use absorbing boundary conditions with $p(r) = 0$ for $r = R_1, R_2$. We solve the diffusion equation

$$\frac{\partial P(r, \phi, t)}{\partial t} = \frac{1}{2} \left(\frac{\partial^2 P}{\partial r^2} + \frac{1}{r} \frac{\partial P}{\partial r} + \frac{1}{r^2} \frac{\partial P}{\partial \phi^2} \right)$$

with the ansatz

$$P(r, \phi, t) = \sum_{n=0}^{\infty} p(r) \cos(n\phi) \exp[-\lambda_n t].$$

For long times, the angular dependence vanishes, and the mode with the slowest decay (the smallest eigenvalue λ_0) dominates. (Note that ϕ is not the winding angle, but the azimuthal angle, which takes only values between 0 and 2π .) Since we normalize the winding angle distribution with respect to the walkers that do not get absorbed, the factor $\exp[-\lambda_0 t]$ drops out, and the probability to find the walker after time t at radius r is given by the solution of

$$\frac{\partial^2 p(r)}{\partial r^2} + \frac{1}{r} \frac{\partial p(r)}{\partial r} + 2\lambda_0 p(r) = 0,$$

with the boundary conditions given above, and with the normalization condition $\int_{R_1}^{R_2} p(r) dr = 1$. The general solution of this (Bessel) differential equation can be written in form of an integral

$$p(r) = \int_0^{\pi} \left[C_1 \cos \left(\sqrt{2\lambda_0} r \sin \zeta \right) + C_2 \cos \left(\sqrt{2\lambda_0} r \cos \zeta \right) \ln \left(\sqrt{2\lambda_0} r \sin^2 \zeta \right) \right] d\zeta.$$

The values of λ_0 , C_1 , and C_2 are obtained by matching two consecutive zeros of this function to $r = R_1$ and $r = R_2$, and by normalizing properly. In general, the solution cannot be

written down in a closed form and has to be found numerically. In the case $R_1 \ll R_2$, the values of λ_0 and C_1/C_2 can be found analytically, since $C_1 \gg C_2$ in this limit, and the first two zeros of $p(r)$ are given by the conditions $\ln(\sqrt{2\lambda_0}R_1) = C_1/C_2$ and $\sqrt{2\lambda_0}R_1 \simeq 2.4$ (the first zero of the Bessel function J_0). In the limit $R_2 - R_1 \ll 1$, we find $p(r) = C \sin\left(\pi \frac{r-R_1}{R_2-R_1}\right)$, where C is the normalization constant.

Exercise: Set $R_1 = 1$ and determine numerically the variance

$$\frac{1}{a} = \int_{R_1}^{R_2} \frac{p(r)dr}{r^2}$$

as a function of R_2 .

B. Polymer bound to an attractive winding center

A polymer can also be confined by an attractive winding center (see Fig. 12): A DP subject to an attractive potential of radius b_0 and binding energy U_0 per unit length, is bound to that winding center. For temperatures above the crossover value of $T^* \propto b_0 \sqrt{U_0}$, the polymer is only weakly bound and wanders horizontally over a large localization length, $l_\perp(T) \simeq b_0 \exp[(T/T^*)^2]$ [8]. The mean vertical distance l_z between consecutive intersections of the polymer with the defect is consequently proportional to l_\perp^2 . Over this distance, the polymer can be approximated by a directed walk which returns to its starting point (the winding center) after a time l_z .

Using the result in Eq. (14), we can derive the winding angle distribution $p_A^o(\tilde{x})$ for such confined random walks. Each walk that returns to its starting point after time t (in the z -plane) is composed of two walks of length $t/2$ going from the starting point to $z(t/2)$. As we have seen in subsection II A, almost all walks of length $t/2$, when mapped on the plane $2\zeta/\ln(t/2)$, have their endpoint on a vertical wall at distance one from the origin. The winding angle distribution for these walks is given by Eq. (14), with t replaced by $t/2$. The probability that a walk that returns to its starting point has a winding angle θ is therefore obtained by adding the probabilities of all combinations of two walks of length $t/2$ whose winding angles add up to θ , i.e.

$$\begin{aligned}
p_A^o(\tilde{x}) &= \int_{-\infty}^{\infty} dy \frac{\pi}{4 \cosh^2(\pi y)} \frac{\pi}{4 \cosh^2(\pi(\tilde{x} - y))} \\
&= \frac{\pi}{2 \sinh^2(\pi \tilde{x}/2)} \left(\frac{\pi \tilde{x}}{2} \coth\left(\frac{\pi \tilde{x}}{2}\right) - 1 \right),
\end{aligned} \tag{21}$$

where $\tilde{x} = 2\theta / \ln(t/2R^2)$.

For large $\tilde{x} \approx x$, the above expression decays as $x \exp[-\pi x]$. A polymer of length t is roughly broken up into t/l_z segments between contacts with the attractive columnar defect. We can assume that the winding angle of each segment is independently taken from the probability distribution in Eq. (21) with $t \approx l_z$. Adding the winding angle distributions of all segments leads to a Gaussian distribution centered around $\theta = 0$, and with a variance proportional to $L \ln(l_z)/l_z$.

C. Confined polymers winding around chiral centers

When the winding center has a chiral asymmetry, the mean winding angle is increased by some finite amount $\Delta\theta$ per unit time. The winding angle distribution is consequently modified to

$$p_c(\theta) = \exp\left[-\tilde{a}(\theta - t\Delta\theta)^2/t\right],$$

with a mean winding angle proportional to the length of the polymer (see also [20]). $1/\tilde{a}$ is larger than $1/a$, since the variances in the number of returns to the winding center, and in $\Delta\theta$, both contribute to the variance of the winding angle. For weak chirality, $1/\tilde{a}$ is close to $1/a$, and the main effect of the chirality is just a shift of winding angle distribution. For strong chirality, we expect $1/\tilde{a} \gg 1/a$, and the winding angle distribution becomes very broad (similar to the situation discussed in section IID).

When the polymer is confined not by a container but by neighboring polymers, it will not just wind around one of these neighbors. Kamien and Nelson [22] have shown that when chirality is strong, screw dislocations proliferate throughout the polymer crystal.

IV. WINDING ANGLES IN RANDOM MEDIA AND FOR SELF-AVOIDING POLYMERS

So far, we only considered winding topologies that can be mapped on ideal random walks. However, when the medium in which the polymer is embedded is non homogeneous, the energies of different polymer configurations are different. Examples are polymers in gels and porous media [23], or magnetic flux lines in high- T_c superconductors, pinned by oxygen impurities [21]. We consider the case of *quenched* randomness, where one end of the polymer is fixed [24].

The behavior of a DP in the presence of short-range correlated randomness is modeled by a directed path on a lattice with random bond energies [25]. In 3 or less dimensions, the polymer is always pinned at sufficiently long length scales. An important consequence of the pinning is that the path wanders away from the origin much more than a random walk, its transverse fluctuations scaling as t^ν , where $\nu \approx 0.62$ in three dimensions, and $\nu = 2/3$ in two dimensions [26,27]. The probability of such paths returning to the winding center are thus greatly reduced, and the winding probability distribution is expected to change.

We examined numerically the windings of a directed path along the diagonal of a cubic lattice (see Fig. 5). To each bond of this lattice was assigned an energy randomly chosen between 0 and 1. Since the statistical properties of the pinned path are the same at finite and zero temperatures, we determined the winding angle of the path of minimal energy by a transfer matrix method. For each realization of randomness, this method [25] finds the minimum energy of all paths terminating at different points, and with different winding numbers. This information is then updated from one time step to the next. From each realization we thus extract an optimal angle as a function of t . The probability distribution is then constructed by examining 2700 different realizations of randomness. To improve the statistics, we averaged over positive and negative winding angles.

The resulting distribution is shown in figure 13, with a scaling variable $x = \theta/2\sqrt{\ln t}$. This scaling form is motivated by that of self-avoiding walks, which in two dimensions follow

a Gaussian distribution

$$p_{SA} \left(x = \frac{\theta}{2\sqrt{\ln t}} \right) = \frac{1}{\sqrt{\pi}} \exp \left(-x^2 \right). \quad (22)$$

The result of the data collapse in Fig. 13 agrees well with the Gaussian distribution

$$p_{\text{rand}} \left(x = \frac{\theta}{2\sqrt{\ln t}} \right) = \sqrt{\frac{1.5}{\pi}} \exp \left(-1.5x^2 \right). \quad (23)$$

Directed paths in random media and self-avoiding walks share a number of features which make the similarity in their winding angle distributions plausible. Both walks meander away with an exponent larger than the random walk value of 1/2. (The exponent of 3/4 for self-avoiding walks is larger than $\nu \approx 0.62$ for polymers in 3 dimensions.) As a result, the probability of returns to the origin is vanishingly small in the limit $t \rightarrow \infty$ for both types of paths, and the properties of the winding center are expected to be irrelevant. (A simple scaling argument suggests that the number of returns to the origin scale as $N(t) \propto 1/t^{1-2\nu}$.) The conformal mapping of section II cannot be applied in either case: The density and size of impurities in a random medium become coordinate dependent under this mapping, as does the excluded volume effect. The winding angle distribution for self-avoiding walks in Eq. (22) has been calculated using a more sophisticated mapping [9,13]. As a similar exact solution is not currently available for polymers in random media, we resort to the scaling argument presented next.

Let us divide the self-avoiding walk, or the directed path, in segments going from $t/2$ to t , from $t/4$ to $t/2$, etc., down to some cutoff length of the order of the lattice spacing, resulting in a total number of segments of the order of $\ln t$ (see Fig. 14). The statistical self-similarity of the walks suggests that a segment of length $t/2^n$ can be mapped onto a segment of length $t/2^{n+1}$ after rescaling by a factor of $1/2^\nu$. Under this rescaling, the winding angle is (statistically speaking) conserved, and consequently all segments have the same winding angle distribution. Convoluting the winding angle distributions of all segments, and assuming that the correlations between segments do not invalidate the applicability of the central limit theorem, leads to a Gaussian distribution with a width proportional to $\ln t$.

This argument does not work for the random walks considered in section II, since the finite radius of the winding center is a relevant parameter. Different segments of the walk are therefore not statistically equivalent, as they see a winding center of different radius after rescaling.

In the pure system, we had to distinguish between repulsive, neutral, and chiral winding centers. Since in the presence of point impurities the polymer does not return to the winding center as often, these differences are now irrelevant. In fact, it can be shown that even an attractive force between the winding center and the polymer cannot bind the polymer to the winding center, as long as it does not exceed some finite threshold [28]. Perhaps not surprisingly, the main conclusion of this section is that the pinning to point randomness decreases entanglement.

V. DISCUSSION AND CONCLUSIONS

Topological entanglements present strong challenges to our understanding of the dynamics of polymers and flux lines. In this paper, we examined the windings of a single directed polymer around a columnar winding center, or the winding of two DPs around each other. By focusing on even this simple physical situation we were able to uncover a variety of interesting properties: The probability distributions for the winding angles can be classified into a number of universality classes characterized by the presence or absence of underlying symmetries or boundary conditions.

For free DPs in a homogeneous medium, we find a number of exponentially decaying distributions: If there is no interaction at all between the polymer and the winding center (corresponding to reflecting boundaries for random walks) we obtain the distribution in Eq. (17). Removing this conservation (absorbing boundaries or repulsive interaction between the polymer and the winding center) leads to the distribution in Eq. (14) whose tails decay twice as fast.

A completely new set of distributions is obtained for chirally asymmetric situations,

where the polymer is preferentially twisted in one direction at the winding center. These distributions have asymmetric exponential tails, with decay constants that depend on the degree of chirality. Strong chirality appears to lead to quite broad distributions. A remaining challenge is to find the complete form of this probability distribution by solving the two dimensional diffusion equation with moving boundary conditions.

When the polymer is confined to a finite volume around the winding center, the winding angle distribution becomes Gaussian, with a width proportional to the length of the polymer. In the presence of chiral asymmetry, the mean winding angle is proportional to the length of the polymer, and we have to distinguish again between the limits of weak and strong chirality.

For non-ideal walks, with a vanishing probability to return to the origin, the properties of the winding center are expected to be irrelevant. Both self-avoiding walks in $d = 2$ dimensions, and polymers pinned by point impurities in $d = 3$, have wandering exponents ν larger than $1/2$ and fall in this category. We present a scaling argument (supported by numerical data) that in this case the probability distribution has a Gaussian form in the variable $\theta/\sqrt{\ln t}$. Not surprisingly, wandering away from the center reduces entanglement. The characteristic width of the Gaussian form is presumably a universal constant that has been calculated exactly for self-avoiding walks in $d = 2$. It would be interesting to see if this constant (only estimated numerically for the impurity pinned polymers in $d = 3$) can be related to other universal properties of the walk. Changing the correlations of impurities (and hence the exponent ν) may provide a way of exploring such dependence.

There are certainly other universality classes not explored in this paper. For example, we did not consider the case of a long-range interaction between the polymer and the winding center. Also, the mapping of a DP in a nematic solvent on a random walk is correct only to first approximation [4,5]. Due to long-range correlations within the nematic solvent, the number of returns of the polymer to the winding center does not increase with $\ln t$, but with $\ln(\ln t)$ for very large t .

The results of this paper also provide conjectures for the winding of non directed polymers

around a rod. If the self-interaction of the polymer can be neglected for some reason, the results of section II can be applied, the parameter τ now being the internal coordinate of the polymer. To first approximation, this might be correct for a polymer close to the θ -point, but three-point interactions which ultimately swell the θ -polymer will eventually invalidate the result [2].

When the polymer swells to give $\nu > 1/2$, as is the case for a self-avoiding random walk in three dimensions, the winding center is no longer important. The projection into the plane perpendicular to a rod is a walk that wanders away from the winding center faster than an ideal random walk. We can therefore apply the results of section IV and conclude that the winding angle distribution is a Gaussian, with a variance proportional to $\ln t$. When the polymer is in the collapsed state, its winding angle distribution is again different, and has still to be found. Since collapsed polymers are relatively compact, they can be approximated by Hamiltonian walks that visit each site within a volume of the size of the polymer exactly once [29,30]. We thus conclude this review with the open problem of determining the probability distribution for windings in the collapsed state by examining the behavior of Hamiltonian walks.

ACKNOWLEDGMENTS

We thank M.E. Fisher, A. Grosberg, Y. Kantor, P. LeDoussal, and S. Redner for helpful discussions. BD is supported by the Deutsche Forschungsgemeinschaft (DFG) under Contract No. Dr 300/1-1. MK acknowledges support from NSF grant number DMR-93-03667.

[1] P. G. de Gennes, *J. Chem. Phys.* **55**, 572 (1971).

[2] M. Doi and S. F. Edwards, *The theory of polymer dynamics*, (Oxford University Press, New York, 1986).

[3] A. Grosberg and S. Nechaev, *Polymer Topology*, Advances in Polymer Science **106**, 1-29 (Springer Verlag, Berlin 1993).

[4] D. R. Nelson, in *Observation, prediction and simulation of phase transitions in complex fluids*, edited by M. Baus, L. F. Rull, and J. P. Ryckaert (Kluwer, The Netherlands, 1995).

[5] P.-G. de Gennes, in *Polymer liquid crystals*, editors A. Cafieri, W. R. Kringbaum, and R. B. Meyer (Academic, New York, 1982).

[6] D. R. Nelson, Phys. Rev. Lett. **60**, 1973 (1988).

[7] M. Rubinstein and S. P. Obukhov, Phys. Rev. Lett. **65**, 1279 (1990).

[8] D. R. Nelson, in *Phase Transitions and Relaxation in Systems with Competing Energy Scales*, edited by T. Riste and D. C. Sherrington (Kluwer Academic Publishers, Dordrecht, Boston, 1993).

[9] B. Duplantier and H. Saleur, Phys. Rev. Lett. **60**, 2343 (1988).

[10] B. Drossel and Mehran Kardar, Phys. Rev. E **53**, 5861 (1996).

[11] J. Rudnick and Y. Hu, J. Phys. A: Math. Gen. **20**, 4421 (1987).

[12] F. B. Knight, *Essentials of Brownian motion and diffusion* (American Mathematical Society, Providence, Rhode Island, 1981).

[13] H. Saleur, Phys. Rev. E **50**, 1123 (1994).

[14] R. Durett, *Brownian Motion and Martingales in Analysis* (Wadsworth, Inc., Belmont, California, 1984).

[15] F. Spitzer, Trans. Am. Math. Soc. **87**, 187 (1958).

[16] C. Bélisle, Ann. Prob. **17**, 1377 (1989).

[17] J. W. Pitman and M. Yor, Ann. Probab. **14**, 733 (1986).

- [18] A. Comtet, J. Desbois, and C. Monthus, *J. Stat. Phys.* **73**, 433 (1993).
- [19] J. V. Selinger and R. L. B. Selinger, *Phys. Rev. Lett.* **76**, 58 (1996).
- [20] B. Houchmandzadeh, J. Lajzerowicz, and M. Vallade, *Journal de Physique I France* **2**, 1881 (1992).
- [21] G. Blatter, M. V. Feigel'man, V. B. Geshkenbein, A. I. Larkin, and V. M. Vinokur, *Rev. Mod. Phys.* **66**, 1125 (1994).
- [22] R. D. Kamien and D. R. Nelson, *Phys. Rev. E* **53**, 650 (1996).
- [23] G. M. Foo, R. B. Pandey, and D. Stauffer, *Phys. Rev. E* **53**, 3717 (1996).
- [24] P. Le Doussal and J. Machta, *J. Stat. Phys.* **64**, 541 (1991).
- [25] M. Kardar, *Lectures on Directed Paths in Random Media*, Les Houches Summer School on Fluctuating Geometries in Statistical Mechanics and Field Theory, August 1994 (in press, see cond-mat/9411022).
- [26] J. G. Amar and F. Family, *Phys. Rev. A* **41**, 3399 (1990).
- [27] J. M. Kim, A. J. Bray, and M. A. Moore, *Phys. Rev. A* **44**, 2345 (1991).
- [28] L. Balents and M. Kardar, *Phys. Rev. E* **49**, 13 030 (1994).
- [29] H. Orland, C. Itzykson, and C. de Dominicis, *J. Physique Lett.* **46**, L353 (1985).
- [30] V. S. Pande, C. Joerg, A. Y. Grosberg, and T. Tanaka, *J Phys A: Math Gen* **27**, 6231 (1994).

FIG. 1. a) Two directed polymers winding around each other. b) A directed polymer winding around a rod.

FIG. 2. Conformal mapping of the random walk with absorbing boundary conditions, and subsequent rescaling.

FIG. 3. Winding angle distribution for random walks on a square lattice with *reflecting* boundary conditions for $t = 38$ (dot-dashed), 152 (long dashed), 608 (dashed), 2432 (dotted), and 9728 (solid). The horizontal axis is $x = 2\theta/\ln(2t)$. The thick solid line is the analytical result of Eq. (17).

FIG. 4. Winding angle distribution for random walks on a square lattice with *absorbing* boundary conditions. The symbols and the variable x are the same as in the previous figure. The thick solid line is the analytical result of Eq. (14).

FIG. 5. a) Construction of a polymer directed along the (1,1,1)-diagonal of a cubic lattice. b) projection into the plane perpendicular to the (1,1,1)-diagonal. The three sublattices are indicated by different shades of gray.

FIG. 6. Winding angle distribution around the preferred direction for a flux line (directed path) in 3 dimensions for $t = 243$ (dot-dashed), 729 (long dashed), 2187 (dashed), 6561 (dotted), and 19684 (solid). The horizontal axis is $x = 2\theta/\ln(2t)$. The thick solid line is the analytical result of Eq. (14).

FIG. 7. Triangular and square lattices with directed bonds. The winding centers are indicated by a circle o.

FIG. 8. Brownian motion around a rotating winding center.

FIG. 9. Winding angle distribution around the preferred direction for a random walk on a directed triangular lattice for $t = 243$ (dot-dashed), 729 (long dashed), 2187 (dashed), 6561 (dotted), and 19684 (solid). The scaling variable is $x = 2\theta/\ln(2t)$. The thick solid line is the distribution given in Eq. (17).

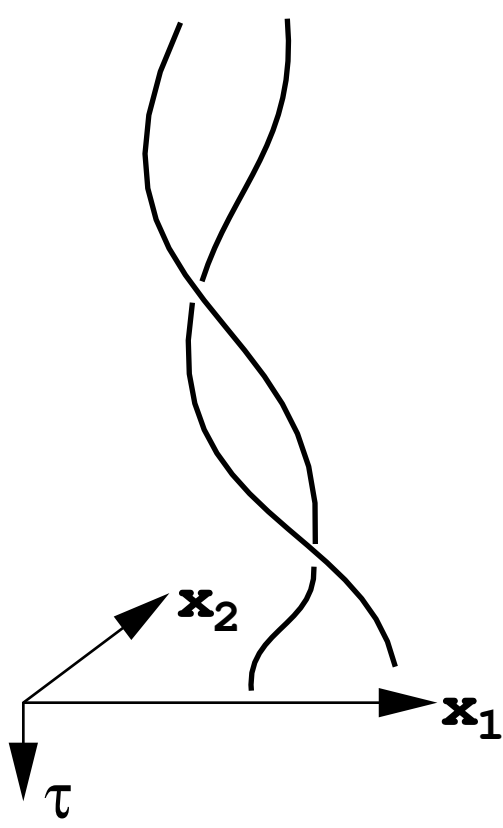
FIG. 10. Winding angle distribution for a random walk on a directed square lattice for $t = 38$ (dot-dashed), 152 (long dashed), 608 (dashed), 2432 (dotted), and 9728 (solid). The thick solid line is the distribution given in Eq. (17).

FIG. 11. A directed polymer confined between two cylinders.

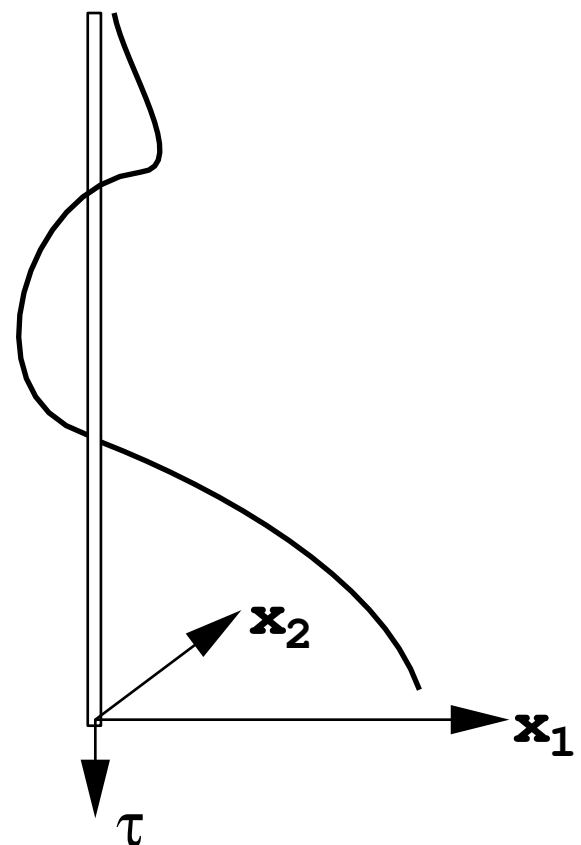
FIG. 12. A directed polymer bound to an attractive rod.

FIG. 13. Winding angle distribution for a directed path in a random 3-dimensional system for $t = 120$ (dotted), 240 (dashed), 480 (long dashed), 960 (dot-dashed), and 1920 (solid). The thick solid line is the Gaussian distribution in Eq. (23).

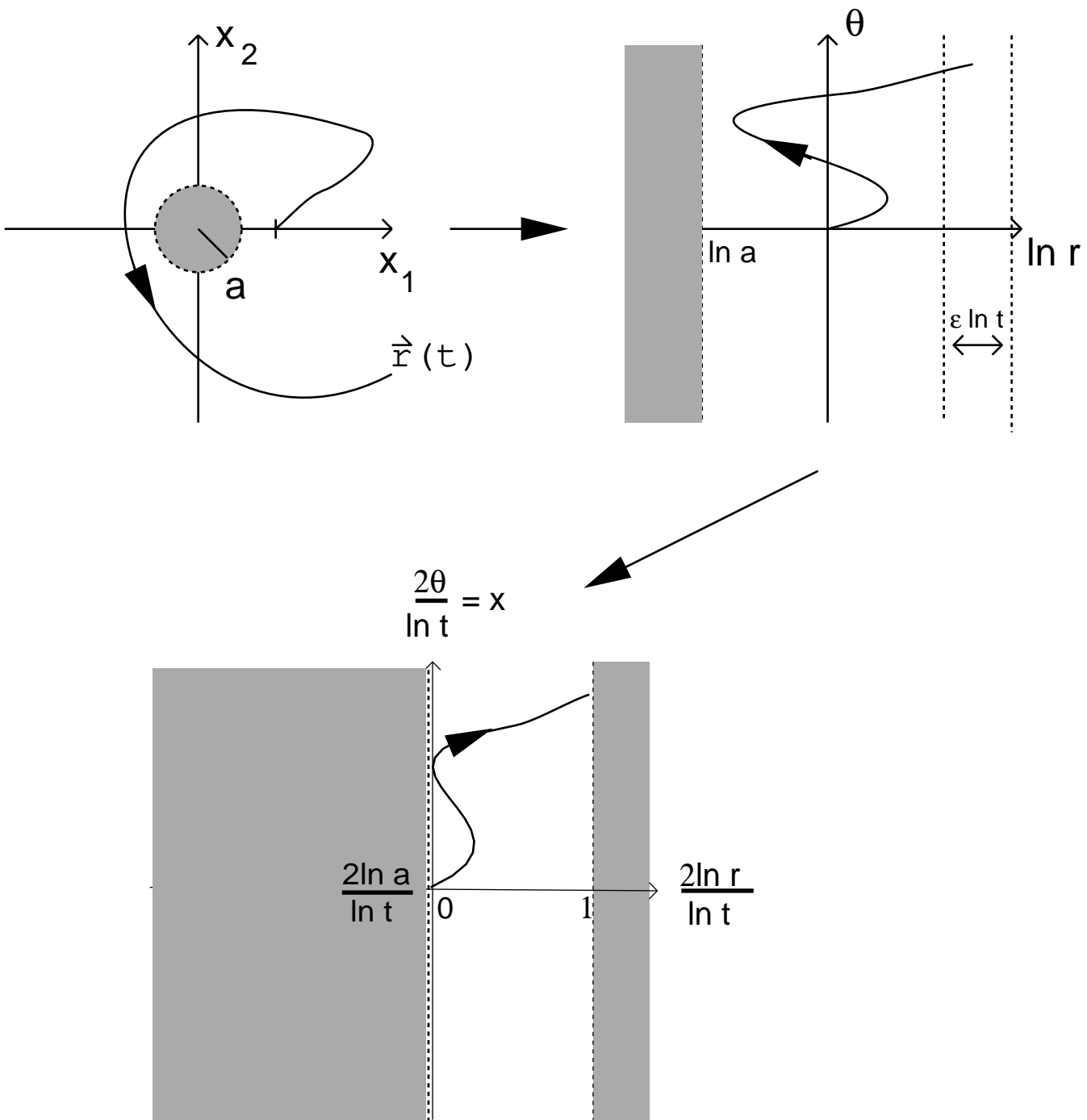
FIG. 14. Division of the self-avoiding walk into self-similar segments.

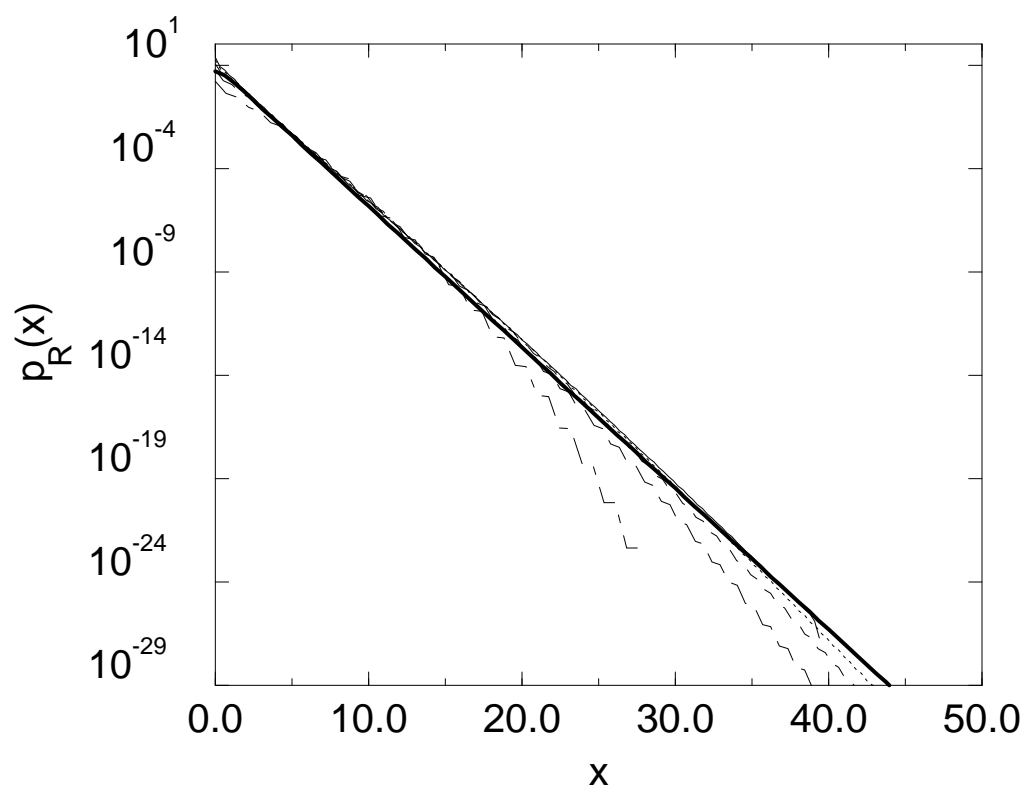


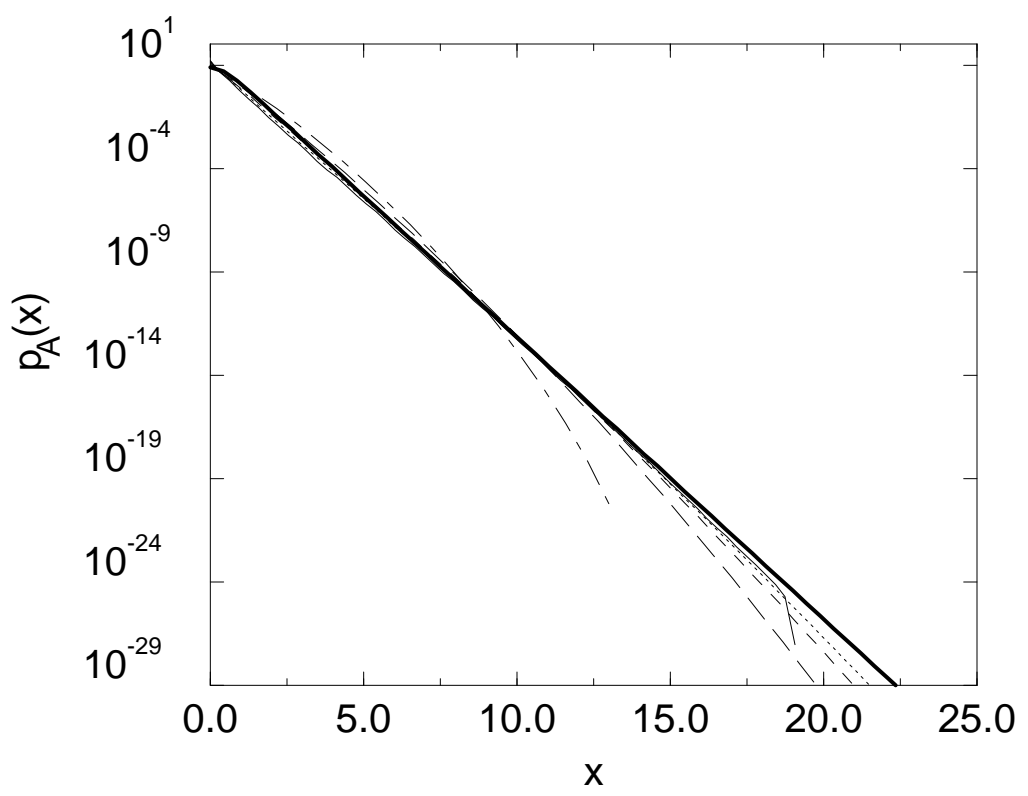
a)

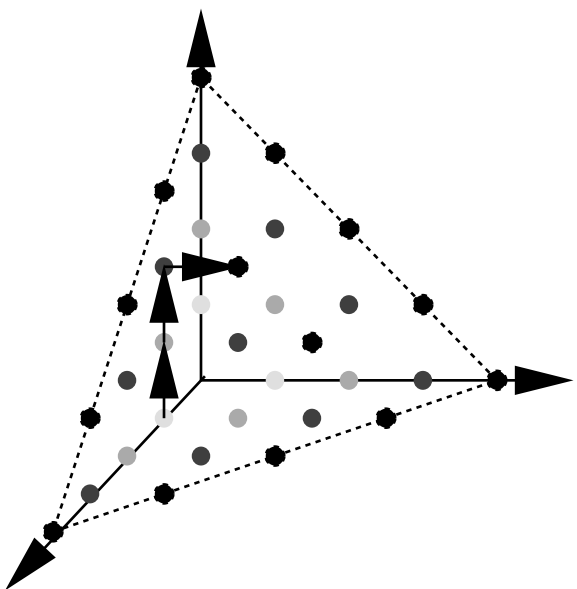


b)

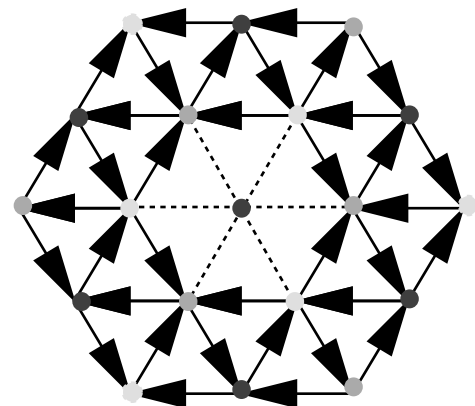




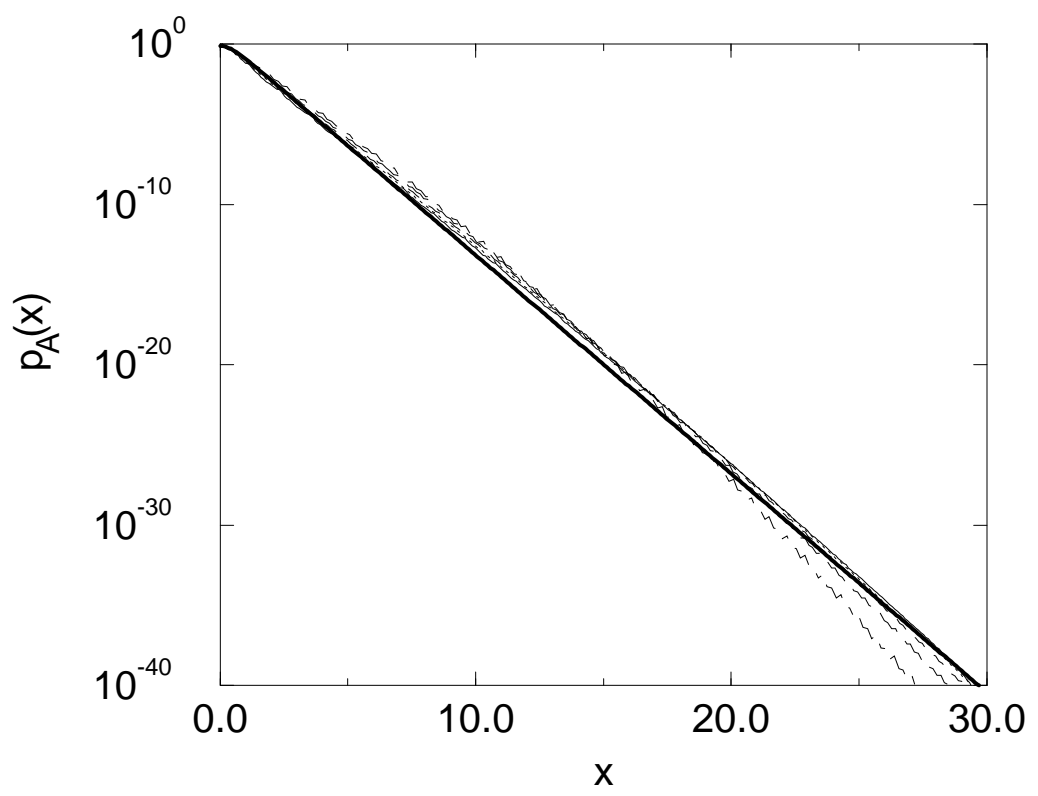


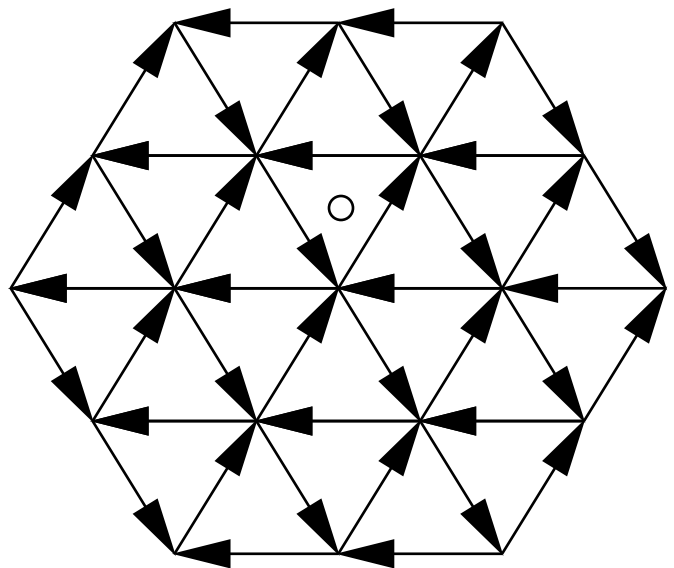


a)

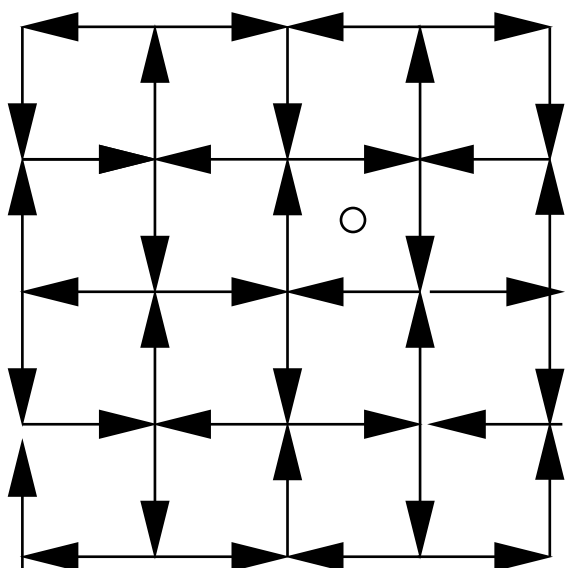


b)





a)



b)

